Ultrasensitive Detection of Dopamine with Carbon Nanopipettes

Keke Hu,[†,‡] Dengchao Wang,[†,≠] Min Zhou,[†,§] Je Hyun Bae,[†] Yun Yu,[†,◊] Huolin Xin,[%] and Michael V. Mirkin[†,‡,]*

†Department of Chemistry and Biochemistry, Queens College, Flushing, NY 11367

‡The Graduate Center of CUNY, New York, NY 10016

≠Present address: School of Chemical Sciences, University of Chinese Academy of Sciences, Beijing 100049, China.

§Present address: Department of Chemistry, Rice University, MS 60, Houston, TX 77005-1892.

◊Present address: Department of Chemistry, University of California, Berkeley, CA 94720.

% Department of Physics & Astronomy, University of California, Irvine, CA 92697.

Corresponding Author
E-mail: mmirkin@qc.cuny.edu
FAX: 718-997-5531

ABSTRACT

Carbon fiber micro- and nanoelectrodes have been extensively used to measure dopamine and other neurotransmitters in biological systems. While the radius of some reported probes was <<1 μm, the length of the exposed carbon was typically on the micrometer scale, thus, limiting the spatial resolution of electroanalytical measurements. Recent attempts to determine neurotransmitters in single cells and vesicles provided additional impetus for decreasing the probe dimensions. Here we report two types of dopamine sensors based on carbon nanopipettes (CNP) prepared by chemical vapor deposition of carbon into the pre-pulled quartz capillary. These include 10 - 200 nm radius CNPs with a cavity near the orifice and CNPs with an open path in the middle, in which the volume of sampled solution can be controlled by the applied pressure. Because of the relatively large surface area of carbon exposed to solution inside the pipette, both types of sensors yielded well-shaped voltammograms of dopamine down to *ca.* 1 nM concentrations, and the unprecedented voltammetric response to 100 pM dopamine was obtained with open CNPs. TEM tomography and numerical simulations were used to model CNP responses. The effect of dopamine adsorption on the CNP detection limit is discussed along with the possibilities of measuring other physiologically important analytes (e.g., serotonin) and eliminating anionic and electrochemically irreversible interferences (e.g., ascorbic acid).

Dopamine (DA) is an important neurotransmitter released by neurons to send signals to other nerve cells.[1] It is stored in sub-micrometer-sized vesicles and eventually ejected into the synaptic cleft (exocytosis).[2,3] The electrochemical detection of DA *in vitro* and *in vivo* is essential for understanding its pathways and functions in nervous system. Wightman and his former students have pioneered the use of carbon ultramicroelectrodes to monitor DA exocytosis.[4-9] Several types of carbon nanotube-based microelectrodes have been fabricated and employed as neurochemical sensors.[10-12]

Smaller (i.e. nm-sized) electrodes are required for intracellular experiments and DA analysis on the level of single vesicles.[13] Carbon nanofibers[13,14] and carbon-coated nanopipettes[15] with a small tip radius have been used to satisfy both requirements; however, the micrometer-scale length of such an electrode limits the spatial resolution and prevents it from being completely inserted into biological vesicles and other small structures. Conical carbon fiber nanoelectrodes prepared by flame-etching micrometer sized carbon fibers were recently applied to neurotransmitter measurements in individual synapses.[16,17] The length of the exposed carbon in these electrodes was also on the micrometer scale. Carbon nanoelectrodes with other geometries, such as sub-micron conical carbon pipes, double-barrel nanoprobes, and carbon ring electrodes, have been prepared by chemical vapor deposition (CVD).[18-22]

Here we discuss two types of carbon nanopipette (CNP) based sensors that combine the small physical size (the tip radius can be <20 nm) with the relatively large surface area of carbon exposed to solution and fast mass transport allowing rapid analysis of the sampled redox species.[23] Prepared by CVD of carbon into the pre-pulled quartz capillaries, they include an "electrochemical nanosampler"[24] with a fixed volume nanocavity near the pipette orifice and open CNPs with an open path in the middle[25] in which the volume of sampled solution can be

controlled by applying pressure. In both cases, the sampling site (i.e. the pipette orifice) is well defined, and cyclic voltammograms (CV) of the redox species sampled in the nanocavity consist of two essentially symmetric peaks produced by their complete oxidation/reduction. The sampled amount of redox species can be quantified by integrating the current under the voltammetric peak.

Even with a simple nanoprobe geometry (e.g., a flat, disk-type nanoelectrode), voltammetric experiments performed without independent characterization of the electrode size/shape and surface morphology are likely to be marred by artifacts and misinterpretations.[26-28] Since CNP geometry is significantly more complicated, thorough characterization is required to enable meaningful experiments with these probes. Additional challenges stem from high complexity of the carbon electrochemistry in general[29,30] and the mechanism of dopamine oxidation in particular.[31] The CNP behavior can be influenced by nature of the CVD carbon (amorphous vs. graphitic), the sp^3/sp^2 ratio and the density of surface oxygen functional groups.[32,33] A recent study employing CNPs for DA sensing[34] focused on fast-scan voltammetry that is more suitable for practical *in vivo* measurements of neurotransmitters than for mechanistic analysis because of a very large contribution of charging current to the measured responses. Here we discuss CNP experiments on a long experimental timescale not suitable for dynamic measurements in living cells. The combination of TEM-based approaches with voltammetry and finite-element simulations is used to analyze the experimental results and elucidate the fundamentals of CNP response to dopamine.

EXPERIMENTAL

Chemicals and Materials. Ferrocenemethanol (FcMeOH; 99%, Alfa Aesar, Haverhill, MA) was sublimed before use. Hexaammineruthenium ($Ru(NH_3)_6Cl_3$) from

Strem Chemicals (Newburyport, MA), dopamine hydrochloride, potassium chloride (≥99 %), potassium ferricyanide, potassium ferrocyanide and phosphate buffered saline (PBS) from Sigma-Aldrich (St. Louis, MO) were used as received. All aqueous solutions were prepared using deionized water from the Milli-Q Advantage A10 system equipped with Q-Gard T2 Pak, a Quantum TEX cartridge and a VOC pak; total organic carbon (TOC) <1 ppb. For all dopamine measurements, pH 7.4 phosphate buffered saline (PBS; 0.137 M NaCl, 0.01 M Na_2HPO_4, and 0.003 M KCl) was prepared by dissolving tablets in deionized water and used as the supporting electrolyte. Dopamine solutions were prepared by diluting stock solution from 2 mM to the desired concentration stepwise with PBS solution. For other measurements, the supporting electrolyte was 0.1 M potassium chloride. 5.0 ultrahigh purity argon and 3.7 ultrahigh purity methane gases (PRAXAIR, Inc.) were used as precursors for CVD.

Fabrication of Carbon Nanopipettes. Quartz capillaries (1.0 mm o.d., 0.5 mm i.d.) were purchased from Sutter Instrument Co. The nanopipettes with the tip radius from 5 to 200 nm were pulled by a laser pipette puller (P-2000; Sutter Instruments) from these quartz capillaries.[25] Different types of carbon nanopipettes were fabricated by controlling the CVD time and the composition of the gas mixture, as described previously.[24,35-37] Briefly, shorter CVD time and smaller ratio of methane to argon produced open CNPs, while longer CVD time and higher methane-to-argon ratio produced either completely filled pipettes or cavity ("nanosampler") CNPs. Other factors, including pipette inside geometry, the furnace temperature, and gas flow rate, can also affect the deposition of the carbon layer.

Characterization of Nanopipettes by TEM. TEM images and tomography of CNPs were acquired using field emission transmission electron microscope (JEOL 2100F) operated at 200 keV. Pipette tip (~3 mm long) was cut off and attached to the grid (PELCO Hole Grids, Copper). The three-dimensional internal structure of the nanopipette tip was reconstructed using electron tomography, a technique that rebuilds 3D structures using a series of projection images from different projection angles. The projection tilt series were recorded from -70 degree to +70 with 2-degree intervals. The 3D reconstructions were rendered using Avizo by isovalue surfaces.

Electrochemical experiments. Voltammetric experiments were performed using a CHI model 760 potentiostat (CH Instruments, Austin, TX). The two-electrode setup was employed with either a commercial Ag/AgCl reference (CHI 111, 1 M KCl) or a 0.25 mm diameter Ag wire coated with AgCl serving as reference electrode. All experiments were carried out at room temperature (22−25 °C) inside a Faraday cage.

Control and calculation of solution volume in a CNP. The integration of the current under the anodic or cathodic peak yields the charge associated with the oxidation/reduction of all redox molecules sampled inside the CNP.[24] The solution volume in the CNP was calculated as the ratio of the charge to bulk concentration of redox species when the adsorption contribution was not significant (see below). In some experiments, the volume of solution inside an open CNPs was controlled by applying positive or negative pressure with a NE-1000 single syringe pump (New Era Pump Systems, Inc. Farmingdale, NY). The pressure value was directly read from the Fisherbrand™ Traceable™ pressure/vacuum gauge (Fisher Scientific) connected between the pump and CNP. After applying pressure, multiple voltammetric cycles were recorded

to monitor the changes in background current. The stabilized charging current indicated that the solution volume inside the pipette reached a stationary value. The quantitative relationship between the solution volume inside the CNP and the charging current is not straightforward.

Finite-element simulations. The electrochemical response of CNPs was modelled diffusion-controlled mass-transport (excess supporting electrolyte) with and without adsorption. The time-dependent and steady-state voltammetric responses were simulated using COMSOL Multiphysics v5.3a (Comsol, Inc.). The axisymmetric diffusion problem for the nanosampler geometry and the COMSOL model report can be found in the Supporting Information.

RESULTS AND DISCUSSION

Voltammetry of dopamine with carbon nanopipettes. When a CNP is immersed in aqueous solution, water gets driven into the pipette by capillary forces. While the nanosampler cavity may get completely filled with solution, the volume inside an open CNP increases with time until it reaches some steady-state value.[24,25] Similar to the previously reported CVs of the outer-sphere redox mediators, exhaustive oxidation of dopamine inside the pipette occurs when the CNP potential (E) is scanned in the anodic direction and its regeneration – during the subsequent cathodic scan (Fig. 1). Both the anodic peak current (i_p; Fig. 1C) and the charge obtained by integrating the oxidation current under the peak (Fig. 1D) are linear functions of dopamine concentration (c_{DA}), and the i_p dependence of on scan rate (v; Figs. 1B,E) is also linear. Linear calibration curves were obtained for c_{DA} values ranging from ~100 nM to a few mM. As long as the solution volume inside the pipette is constant, the charge is proportional to c_{DA} in the external solution. The charge corresponding to the total amount of DA inside the CNP

can be more useful than the i_p value for determining the amount of DA in a single biological vesicle or other single entity analysis.

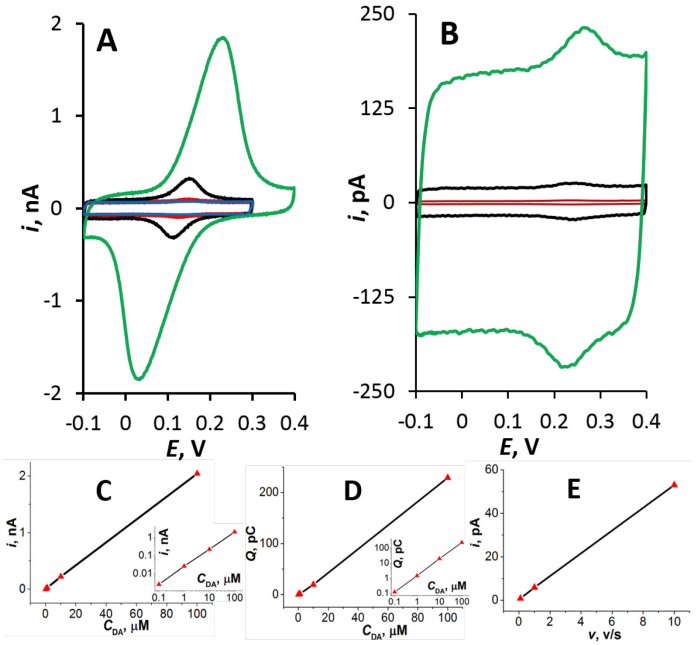

Figure 1. CVs of DA obtained with (A) a nanosampler and (B) an open CNP. The peak current (C) and charge (D) vs. DA concentration calibration curves are from CVs shown in panel A. (E) Scan rate dependence of the peak current for CVs shown in panel B. (A) a = 150 nm, v =0.1 V/s, c_{DA}, µM = 0.1 (blue curve), 1 (red), 10 (black) and 100 (green). (B) a =120 nm, c_{DA} = 1 nM, v, V/s = 0.1 (red),1 (black) and 10 (green). The insets in (C) and (D) show log-log plots of the same data.

Different sampling strategies have to be employed for a nanosampler and an open CNP. Because the cavity of the nanosampler is relatively shallow, the mass-transfer rate is sufficiently fast to sample DA from solution by diffusion. For the cavity depth, h ~1-5 µm, the expected diffusion time is of the order of 0.01 s. Because the solution volume in an open CNP is significantly larger and the mass-transfer in and out of the pipette is relatively slow, the way to quickly sample DA is to draw the solution into the CNP by capillary force or applied pressure. The solution volume inside an open CNP can be controlled by applying the external pressure to it using a syringe pump (Fig. 2). The nine CV cycles in Fig. 2A (v = 0.5 V/s) show the changes in

the voltammetric response of 2 mM ferrocyanide induced by gradually increasing outward pressure applied to the open CNP with the orifice radius, a = 125nm. As the pressure increased, the solution was pushed out of the pipette, and the height of both anodic and cathodic peaks decreased. For each potential cycle, the solution volume can be found from the charge value obtained by integrating the current to produce the volume vs. pressure calibration curve (Fig. 2B). Using such a calibration, the desired solution volume in the pipette can be obtained by applying the corresponding pressure to it.

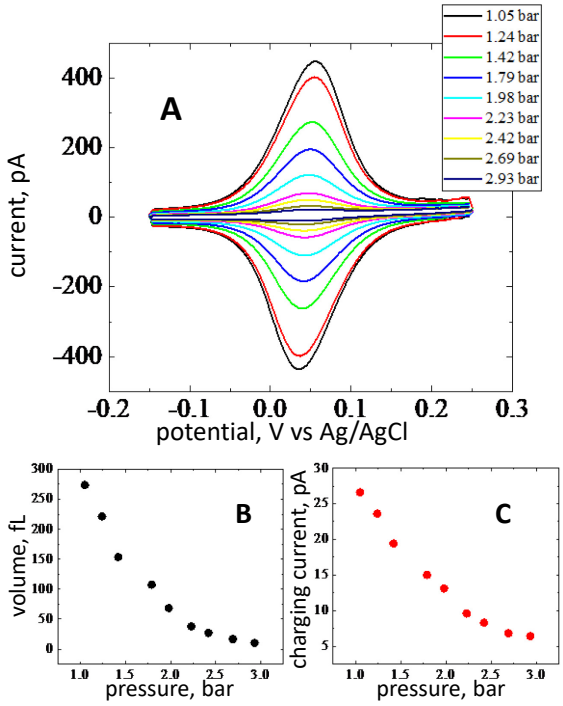

Figure 2. Electrochemical calibration of the open CNP response as a function of the applied pressure. (A) Nine voltammetric cycles of 2 mM ferrocyanide in 0.3 M KCl recorded at an open CNP by gradually increasing the applied outward pressure from 1.05 bar (top) to 2.93 bar (bottom). a = 125 nm. (B) Volume vs. pressure calibration curve obtained from (A). (C) Charging current vs. pressure calibration curve obtained at E = -0.12 V.

When no electrochemical reaction occurs at the CNP (or no redox mediator is added to the solution), the double layer charging current (i_c) can be calibrated vs. the applied pressure

(Fig. 2C) and used to evaluate the area of the carbon film exposed to solution since it is directly proportional to i_c at a given scan rate. However, the interpretation of this dependence is not straightforward because of the microporous structure of the carbon layer. To establish the relationship between the true and geometric surface area of carbon, one needs detailed information about the film thickness and porosity (both quantities presumably vary along the pipette axis), which not currently available. The possibility of significant accumulation of cations inside nanopores and anion exclusion caused by the negative surface charge can also greatly influence CNP electrochemistry.[38]

TEM characterization of CNPs. The information about CNP geometry can be obtained from TEM images and used to quantitatively model the CNPs response. Fig. 3A and Fig. 3B shows TEM images of an open CNP and a nanosampler, respectively. The contrast difference in the open CNP indicates a hollow channel with the ~150 nm diameter at the tip. The rough internal surface and the smooth outer surface suggest that carbon was only deposited on the inner pipette wall (this is important because the external carbon film could contribute to the measured current). The nanosampler CNP in Fig. 3B shows a shallow cavity with $h \approx 300$ nm and $a \approx 30$ nm. Although conventional TEM images provide some information about the CNP depth and diameter, it is limited to a specific two-dimensional projection that may not accurately represent the complicated geometry of the nanocavity.

Electron tomography (see Supplementary Movies) can provide a more detailed and reliable three-dimensional picture of the CNP inside geometry. The two frames from 3D reconstructions along vertical and horizontal axes (Figs. 3C and 3D) of the nanosampler imaged in Fig. 3B clearly show that the narrow shaft of the quartz pipette was compactly

filled with carbon except several nanoscale voids along its axis. These cavities are not connected, and only one of them adjacent to the tip is exposed to solution. The carbon surface is rough and porous. The CNP orifice is essentially circular with ~62 nm diameter, and the thickness of the pipette wall at the tip is ~10 nm.

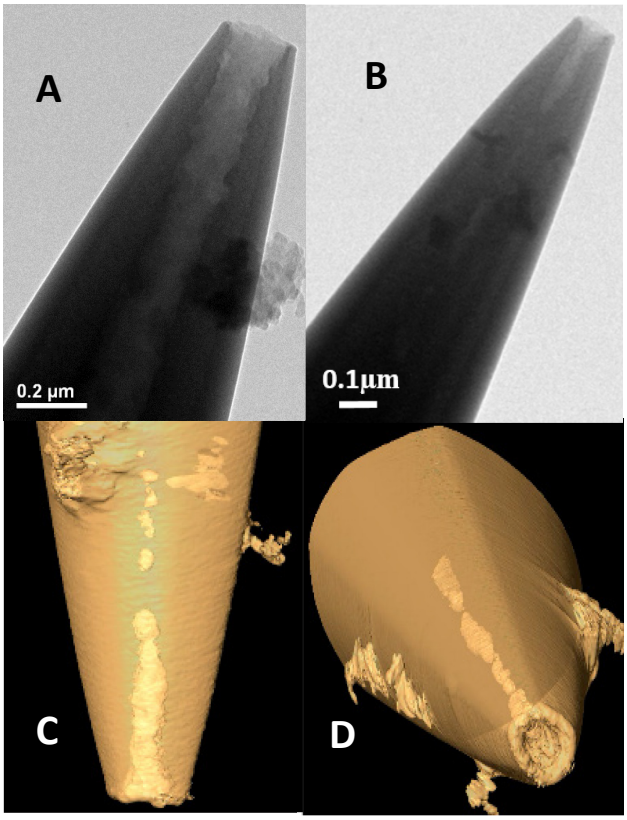

Figure 3. TEM images of (A) open CNP and (B) nanosampler; and (C,D) two frames from tomography movies of the same nanosampler. *a*, nm = 75 (A) and 31 (B).

Detecting ultra-low concentrations of dopamine. CNP CVs obtained with relatively high concentrations of DA (e.g., > ~50 nM) could be quantitatively fit to the diffusion-based simulated curves (Fig. 4A). This observation is accord with the recent findings that surface charge and double-layer effects in CNPs are small when the supporting electrolyte concentration is relatively high (e.g., ~0.1 M), and the accumulation/depletion of single-charged ionic redox species is insignificant.[38] However,

for DA concentrations lower than ~50 nM, the concentration dependence of the i_p becomes nonlinear (Fig. S1), and the CNP voltammetric current and charge became significantly higher than the values predicted by simple diffusion-based simulations.

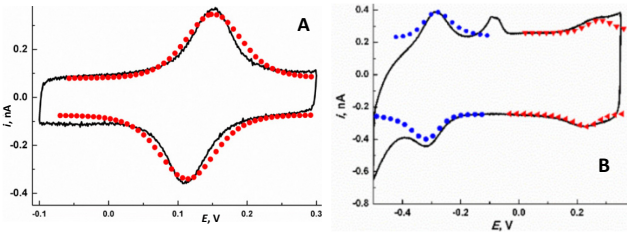

Figure 4. Experimental (solid lines) and simulated (symbols) CNP CVs of 10 μM DA (A) and 100 pM DA + 1 μM $Ru(NH_3)_6Cl_3$ (B) in pH 7.4 PBS. *a*, nm = 200 (A) and 230 (B), *h,* μm = 130 (A) and 345 (B); *v* = 1 V/s. The pipette angle is ~5°.

The voltammogram in Fig. 5A was recorded with an open CNP in solution containing 100 pM DA, i.e. about three orders of magnitude lower than those measured previously by electrochemical techniques. The peak potentials in Fig. 5A correspond to oxidation/reduction of dopamine, while no peaks appear within a broad potential window in the background curve (Fig. 5B) recorded with the same CNP but with no DA in solution. Similar voltammograms have been obtained with other CNPs. Although the faradaic current must be due to dopamine, the amount of charge is much larger than one can expect from 100 pM DA in the solution volume contained inside the pipette shaft.

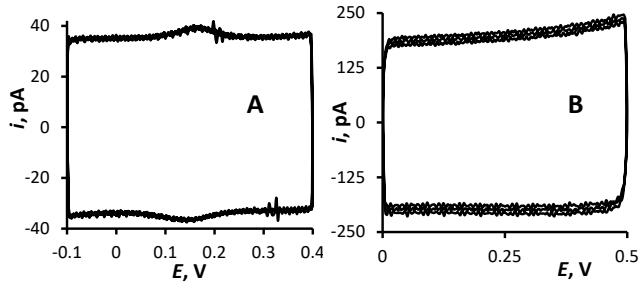

Figure 5. CVs recorded with the same open CNP in PBS solution containing (A) 100 pM DA and (B) no DA. *v*, V/s = 0.1 (A) and 0.5 (B). *a* = 150 nm.

We hypothesize that the adsorption of dopamine on the large surface of nanoporous carbon film may be responsible for this unexpectedly high signal.

The voltammograms in sub-nM DA solutions were obtained using open CNPs that typically exhibit higher sensitivity than nanosamplers due to larger solution volume and carbon surface area. The solution volume needs to be known to elucidate the origins of voltammetric response. Because the solution volume inside an open CNP cannot be validated by TEM, we measured and simulated CVs of the mixture of sub-nM DA and a much higher concentration of $Ru(NH_3)_6Cl_3$ (e.g., 100 pM DA and 1 μM $Ru(NH_3)_6Cl_3$ in Fig. 4B). The pair of cathodic and anodic peaks near -0.3 V correspond to the reduction and oxidation of $Ru(NH_3)_6^{3/2+}$, while the DA peaks appear at ~ +0.2 V. (The origin of the irreversible peak at *ca.* -0.1 V is not known. This peak was observed with different CNPs in solutions simultaneously containing DA and $Ru(NH_3)_6Cl_3$). The total charge found from hexaammineruthenium peaks after background subtraction is 12 pC, corresponding to the solution volume in the CNP *ca.* 120 pL. This volume and other independently determined geometric parameters were used to simulate a CV (blue symbols in Fig. 4B) with a reasonably good agreement between experimental and theoretical peaks of $Ru(NH_3)_6^{3/2+}$. The charge of the complete oxidation of 100 pM DA calculated based on the determined volume is only 2.4 fC, and the corresponding peak current, 0.014 pA, would be immeasurably small.

Since no significant cation preconcentration inside a CNP can be expected in PBS solution (ionic strength >0.1 M), and the electrostatic accumulation of $DA^{+/0}$ ions must be even less significant than that of multi-charged $Ru(NH_3)_6^{3/2+}$,[38] the ~70 pA DA peak current in Fig. 4B is likely due to dopamine adsorption on the large surface of porous

carbon. DA adsorption on various carbon surfaces is well documented.[39-43] The simulated dopamine peaks (red dots) fit the experimental CV in Fig. 4B with the DA surface concentration of 5000 pmol/cm^2. This number is significantly larger than the DA saturation coverage reported earlier, i.e., ~100-1000 pmol/cm^2.[39-43] The difference is consistent with the true surface area of the porous carbon film being much larger than the geometric area of the CNP segment filled with solution. Unlike relatively slow diffusion of dissolved species, oxidation/reduction of adsorbed molecules is not limited by mass-transfer rate.

Further evidence of significant dopamine accumulation within the porous carbon phase comes from comparing CVs obtained before and after immersing a CNP in 10 nM DA solution (Fig. 6). The voltammogram recorded with a 90-nm-radius nanosampler in pH 7.4 PBS (Fig. 6A) is essentially featureless, but well defined anodic and cathodic peaks of dopamine were obtained with the same electrode immersed in 10 nM DA solution (Fig.6B). Then, the same CNP was rinsed with water and spent 30 min in PBS containing no redox mediator to make sure that all DA is removed from the filling solution, and another CV was recorded in blank PBS solution (Fig. 6C) showing both anodic and cathodic DA peaks. The comparable magnitudes of the voltammetric peaks in Figs. 6B and 6C suggest that at the 10 nM concentration, DA molecules adsorbed on the surface of carbon nanopores make a significant contribution to the measured current. The contribution of DA accumulated inside the carbon porous structure becomes more significant as its concentration in solution decreases – it is apparently negligible at micromolar (and submicromolar) concentrations, but largely determines the response when c_{DA} is <1 nM.

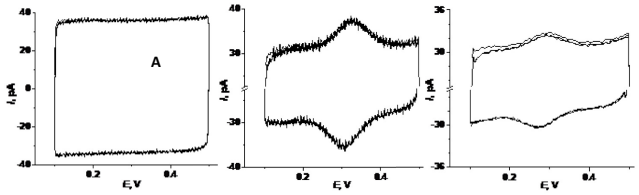

Figure 6. Voltammograms obtained sequentially in pH 7.4 PBS (A), 10 nM DA (B) and pH 7.4 PBS (C) at the same carbon nanosampler. v = 1V/s; a = 90 nm.

A potential issue in detecting low DA concentrations is that some CNP voltammograms obtained in a blank solution exhibited a pair of peaks with the potentials close to those of dopamine peaks (Fig. S2). These peaks are apparently related to oxidation/reduction of carbon–oxygen functionalities. Various voltammetric features due to carbon surface functional groups (e.g., quinone-type species) have been reported in the literature.[44] In our experiments, these peaks were observed with a relatively small number of CNPs. The possibility of this artifact can be eliminated by obtaining a CV in a blank solution before DA voltammetry with the same CNP, as shown in Fig. 5.

Permselectivity, interferences, and other analytes. Two approaches to improving selectivity of DA analysis in the presence of interferences are illustrated by the CNP CVs of DA mixed with ascorbic acid (Fig. 7). Ascorbic acid that is often present in biological samples can interfere with DA analysis because their voltammetric waves significantly overlap.[45] However, the adsorption of DA and significant negative charge density on the carbon surface, resulting in depletion of anionic species and large shifts of peak potentials,[38] can enable quantitative analysis of DA in the presence of a much higher concentration of ascorbic acid (negatively charged at pH 7; pK_{a1} = 4.04). In Fig. 7A obtained with a 28-nm-radius CNP, the anodic peak at -0.05 V produced by irreversible oxidation of 0.1 mM ascorbic acid (curve 1) is only ~7 times higher the reversible peak

produced by 50 nM DA. Moreover, the peaks are well separated, so that ascorbic acid does not significantly interfere with the determination of DA.

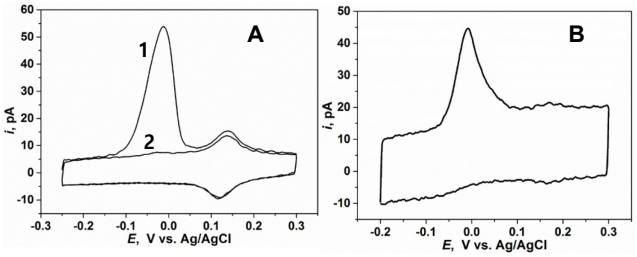

Figure 7. CVs obtained with 28 nm (A) and 260 nm (B) radius CNPs in PBS solution containing 0.1 mM ascorbic acid and 50 nM DA (A), and 0.5 mM ascorbic acid and 5 nM DA (B). v = 0.5 V/s. Curves 1 and 2 in (A) represent the first and the second potential cycles of the same CV.

The irreversibility of the ascorbic acid oxidation can also improve the selectivity of DA analysis using CNPs. The anodic peak of ascorbic acid prominent in the first voltammetric cycle (curve 1 in Fig. 7A) almost completely disappeared in the next cycle (curve 2) because the oxidation is irreversible and the mass transport from the outer solution into the CNP is relatively slow. With the concentration ratio as large as 10^5 (i.e. 0.5 mM ascorbic acid and 5 nM DA) and a larger CNP radius (a = 260 nm), the higher ascorbic acid peak still does not obliterate the DA peaks in the second potential cycle of the CV shown in Fig. 7B. This level of selectivity against ascorbic acid is essential for biomedical applications since the concentrations of DA in human serum are within the nM range,[46] while the corresponding ascorbic acid concentrations can be *ca.* 0.2– 0.5 mM.[47] By contrast, the ten-fold higher concentration of ascorbic acid completely obscured the voltammetric wave of DA at a conventional carbon microdisk electrode either under steady-state conditions (Fig. S3A) or in fast-scan CV (v = 500 V/s; Fig. S3B) and made DA detection problematic even by differential pulse voltammetry (Fig. S3C).

The above approaches should be useful for eliminating charged and/or irreversible interferences and improving selectivity of CNP sensors for different analytes. Similarly, the adsorption and/or cation accumulation inside the nanocavity can enable ultra-sensitive detection of physiologically important species other than dopamine. For instance, Fig. 8A shows a well-shaped voltammogram of 10 nM serotonin – another neurotransmitter whose *in vivo* electroanalysis is known to be challenging.[48] The background curve obtained with the same CNP under the same experimental conditions but with no serotonin in solution is shown for comparison in Fig. 8B.

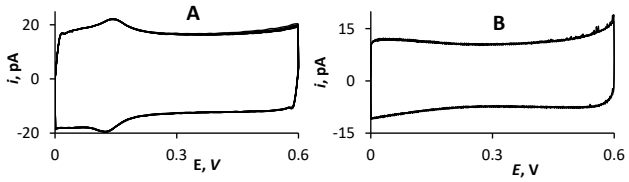

Figure 8. Voltammogram of 10 nM serotonin in pH 7.4 PBS (A) and corresponding background CV obtained with the same open CNP (B). a =150 nm, v = 1 V/s.

CONCLUSIONS

The small physical size, relatively large conductive surface area, and well-defined sampling location make open CNPs and carbon nanocavity electrodes useful for dopamine electroanalysis. We used the combination of voltammetry, TEM and finite-element simulations to investigate CNP response to DA and elucidate the origins of its high sensitivity and selectivity. Two distinct regimes have been identified: diffusion-controlled, complete oxidation/reduction of dopamine molecules contained in the pipette shaft with the peak current and total charge proportional to c_{DA} in the bulk solution at relatively high (e.g., >50 nM) concentrations, and the non-linear response occurring at lower concentrations. Unlike recent experiments in which significant accumulation of cations and depletion of anions inside CNPs were observed only in weakly supported

media (i.e. with 0.1 - 1 mM supporting electrolyte), the response to low concentrations of DA is greatly enhanced by its adsorption on the surface of porous carbon layer at high electrolyte concentrations (e.g., 0.1 M). This effect enabled the detection of 100 pM DA that would have produced immeasurably low current if the mass-transfer of DA was diffusion limited. Additionally, the greatly improved selectivity of CNP voltammetric analysis can be attained by suppressing electrochemically irreversible intermediates; for example, DA could be measured in the presence of 10^5 times higher concentration of ascorbic acid. Similarly high sensitivity and selectivity can be expected for serotonin and other analytes adsorbed on carbon.

ASSOCIATED CONTENT

Supporting Information. Additional voltammograms of DA, supplementary movies showing 3D visualization of the carbon nanosampler, time-dependent diffusion problem, and COMSOL simulation report. This material is available free of charge via the Internet at http://pubs.acs.org.

AUTHOR INFORMATION

Corresponding Author

*E-mail: mmirkin@qc.cuny.edu

Author Contributions

All authors have given approval to the final version of the manuscript.

Notes

The authors declare no competing financial interest.

ACKNOWLEDGMENTS

The support of this work by the National Science Foundation (CHE-1763337) is gratefully

acknowledged. This research used resources of the Center for Functional Nanomaterials, which is a U.S. DOE Office of Science Facility, at Brookhaven National Laboratory under Contract No. DE-SC0012704.

REFERENCES

1. Romanelli, R.J.; Williams, J.T.; Neve, K.A. Dopamine receptor signaling: intracellular pathways to behavior. In Neve, K.A., ed. The Dopamine Receptors. Springer: 2009, pp 137–174.
2. Alvarez de Toledo, G.; Fernandez-Chacon, R; Fernandez, J.M. Release of secretory products during transient vesicle fusion. *Nature* **1993**, *642*, 554–558.
3. Stevens, C. F. Neurotransmitter release at central synapses. *Neuron* **2003**, *40*, 381 – 388.
4. Ewing, A. G.; Bigelow, J. C.; Wightman, R. M. Direct in vivo monitoring of dopamine released from two striatal compartments in the rat. *Science* **1983**, *221*, 169-171.
5. Ewing, A. G.; Strein, T. G.; Lau, Y. Y. Analytical chemistry in microenvironments: single nerve cells. *Acc. Chem. Res.* **1992**, *25*, 440-447.
6. Bucher, E. S.; Wightman, R. M. Electrochemical Analysis of Neurotransmitters. *Annu. Rev. Anal. Chem.* **2015**, *8*, 239-261.
7. Walters, S. H.; Robbins, E. M.; Michael, A. C. Kinetic Diversity of Striatal Dopamine: Evidence from a Novel Protocol for Voltammetry. *ACS Chem. Neurosci.* **2016**, *7*, 662– 667.
8. Yang, C.; Trikantzopoulos, E.; Nguyen, M. D.; Jacobs, C. B.; Wang, Y.; Mahjouri-Samani, M.; Ivanov, I. N.; Venton, B. J., Laser Treated Carbon Nanotube Yarn

Microelectrodes for Rapid and Sensitive Detection of Dopamine in Vivo. *ACS Sensors* **2016**, *1*, 508−515.

9. Roberts, J.G.; Sombers, L. A. Fast Scan Cyclic Voltammetry: Chemical Sensing in the Brain and Beyond. *Anal. Chem.* **2018**, *90*, 490-504.
10. Swamy, B. E. K.; Venton, B. J. Carbon nanotube-modified microelectrodes for simultaneous detection of dopamine and serotonin in vivo. *Analyst* **2007**, *132*, 876−884.
11. Harreither, W.; Trouillon, R.; Poulin, P.; Neri, W.; Ewing, A. G.; Safina, G. Carbon Nanotube Fiber Microelectrodes Show a Higher Resistance to Dopamine Fouling. *Anal. Chem.* **2013**, *85*, 7447−7453.
12. Yang, C.; Jacobs, C. B.; Nguyen, M. D.; Ganesana, M.; Zestos, A. G.; Ivanov, I. N.; Puretzky, A. A.; Rouleau, C. M.; Geohegan, D. B.; Venton, B. J. Carbon Nanotubes Grown on Metal Microelectrodes for the Detection of Dopamine. *Anal. Chem.* **2016**, *88*, 645−652.
13. Li, X.; Majdi, S.; Dunevall, J.; Fathali, H.; Ewing, A. G. Quantitative measurement of transmitters in individual vesicles in the cytoplasm of single cells with nanotip electrodes. *Angew. Chem. Int. Ed.* **2015**, *54*, 11978-11982.
14. Phan, N. T. N.; Li, X.; Ewing, A. G. Measuring synaptic vesicles using cellular electrochemistry and nanoscale molecular imaging. *Nat. Rev. Chem.* **2017**, *1*, 0048.
15. Rees, H. R.; Anderson, S. E.; Privman, E.; Bau, H. H.; Venton, B. J. Carbon nanopipette electrodes for dopamine detection in Drosophila. *Anal. Chem.* **2015**, *87*, 3849-3855.

16. Li, Y. T.; Zhang, S. H.; Wang, L.; Xiao, R. R.; Liu, W.; Zhang, X. W.; Zhou, Z.; Amatore, C.; Huang, W. H. Nanoelectrode for amperometric monitoring of individual vesicular exocytosis inside single synapses. *Angew. Chem. Int. Ed.* **2014**, *53*, 12456-12460.
17. Li, Y.T.; Zhang, S.H.; Amatore, C.; Huang, W.H. Real-time Monitoring of Discrete Synaptic Release Events and Excitatory Potentials within Self-reconstructed Neuromuscular Junctions. *Angew. Chem. Int. Ed.* **2015**, *54*, 9313 –9318.
18. Kim, B. M.; Murray, T.; Bau, H. H. The fabrication of integrated carbon pipes with sub-micron diameters. *Nanotechnology* **2005**, *16*, 1317–1320.
19. Singhal, R.; Bhattacharyya, S.; Orynbayeva, Z.; Vitol, E.; Friedman, G.; Gogotsi, Y. Small diameter carbon nanopipettes. *Nanotechnology* **2010**, *21*, 15304.
20. Takahashi, Y.; Shevchuk, A. I.; Novak, P.; Zhang, Y.; Ebejer, N.; Macpherson, J. V.; Unwin, P. R.; Pollard, A., J.; Roy, D.; Clifford, C. A.; Shiku, H.; Matsue, T.; Klenerman, D.; Korchev, Y. E. Multifunctional nanoprobes for nanoscale chemical imaging and localized chemical delivery at surfaces and interfaces. *Angew. Chem., Int. Ed.* **2011**, *50*, 9638-9342.
21. Thakar, R.; Weber, A. E.; Morris, C. A.; Baker, L. A. Multifunctional carbon nanoelectrodes fabricated by focused ion beam milling. *Analyst* **2013**, *138*, 5973-5982.
22. Wilde, P.; Quast, T.; Aiyappa, H. B.; Chen, Y. T.; Botz, A.; Tarnev, T.; Marquitan, M.; Feldhege, S.; Lindner, A.; Andronescu, C.; Schuhmann, W. Towards Reproducible Fabrication of Nanometre-Sized Carbon Electrodes: Optimisation of Automated Nanoelectrode Fabrication by Means of Transmission Electron Microscopy. *ChemElectroChem* **2018**, *5*, 3083-3088.

23. Yu, R.-J.; Ying, Y.-L.; Gao, Rui; Long, Y.-T. Confined Nanopipette Sensing: From Single Molecules, Single Nanoparticles, to Single Cells. *Angew. Chem., Int. Ed.* **2019**, *58*, 3706-3714.
24. Yu, Y.; Noël, J.-M.; Mirkin, M. V.; Gao, Y.; Mashtalir, O.; Friedman, G.; Gogotsi, Y. Carbon Pipette-Based Electrochemical Nanosampler. *Anal. Chem.* **2014**, *86*, 3365-3372.
25. Hu, K.; Wang, Y.; Cai, H.; Mirkin, M. V.; Gao, Y.; Friedman, G.; Gogotsi, Y. Open Carbon Nanopipettes as Resistive-Pulse Sensors, Rectification Sensors and Electrochemical Nanoprobes. *Anal. Chem.* **2014**, *86*, 8897-8901.
26. Baranski, A. S. On Possible Systematic Errors in Determinations of Charge Transfer Kinetics at Very Small Electrodes. *J. Electroanal. Chem.* **1991**, *307*, 287-292.
27. Nogala, W.; Velmurugan, J.; Mirkin, M. V. Atomic Force Microscopy of Electrochemical Nanoelectrodes. *Anal. Chem.* **2012**, *84*, 5192-5197.
28. Nioradze, N.; Chen, R.; Kim, J.; Shen, M.; Santhosh, P.; Amemiya, S. Origins of Nanoscale Damage to Glass-Sealed Platinum Electrodes with Submicrometer and Nanometer Size. *Anal. Chem.* **2013***, 85*, 6198-6202.
29. McCreery, R.L. Advanced carbon electrode materials for molecular electrochemistry. *Chem. Rev.* **2008**, *108*, 2646-2687.
30. Radovic, L.R. Surface chemical and electrochemical properties of carbons. In Carbons for electrochemical energy storage and conversion systems. CRC Press: 2016, pp 163-219.

31. Muguruma, H.; Inoue, Y.; Inoue, H.; Ohsawa, T. Electrochemical Study of Dopamine at Electrode Fabricated by Cellulose-Assisted Aqueous Dispersion of Long-Length Carbon Nanotube. *J. Phys. Chem. C* **2016**, *120*, 12284–12292.

32. Roberts, J.G.; Moody, B.P.; McCarty, G.S.; Sombers, L.A. Specific oxygen-containing functional groups on the carbon surface underlie an enhanced sensitivity to dopamine at electrochemically pretreated carbon fiber microelectrodes. *Langmuir* **2010**, *26*, 9116-9122.

33. Sainio, S.; Nordlund, D.; Caro, M. A.; Gandhiraman, R.; Koehne, J.; Wester, N.; Koskinen, J.; Meyyappan, M.; Laurila, T. Correlation between sp^3-to-sp^2 Ratio and Surface Oxygen Functionalities in Tetrahedral Amorphous Carbon (ta-C) Thin Film Electrodes and Implications of Their Electrochemical Properties. *J. Phys. Chem. C* **2016**, *120*, 8298−8304.

34. Yang, C.; Hu, K.; Wang, D.; Zubi, Y.; Lee, S. T.; Puthongkham, P.; Mirkin, M. V.; Venton, B. J. Cavity Carbon Nanopipette Electrodes for Dopamine Detection. *Anal. Chem.* **2019**, *91,* 4618−4624.

35. Vitol, E. A.; Schrlau, M. G.; Bhattacharyya, S.; Ducheyne, P.; Bau, H. H.; Friedman, G.; Gogotsi, Y. Effects of Deposition Conditions on the Structure and Chemical Properties of Carbon Nanopipettes. *Chem. Vap. Deposition* **2009**, *15*, 204-208.

36. Singhal, R.; Bhattacharyya, S.; Orynbayeva, Z.; Vitol, E.; Friedman, G.; Gogotsi, Y. Small diameter carbon nanopipettes. *Nanotechnology* **2009**, *21*, 015304.

37. Hu, K.; Gao, Y.; Wang, Y.; Yu, Y.; Zhao, X.; Rotenberg, S. A.; Gökmeşe, E.; Mirkin, M. V.; Friedman, G.; Gogotsi, Y. Platinized Carbon Nanoelectrodes as Potentiometric and Amperometric SECM Probes. *J. Solid State Electrochem.* **2013**, *17*, 2971-2977.

38. Bae, J. H.; Wang, D.; Hu, K.; Mirkin, M. V. Surface Charge Effects on Voltammetry in Carbon Nanocavities. *Anal. Chem.* **2019**, *91*, 5530–5536.

39. Anjo, D. M.; Kahr, M.; Khodabakhsh, M.; Nowinski, S.; Wanger, M. Electrochemical Activation of Carbon Electrodes in Base: Minimization of Dopamine Adsorption and Electrode Capacitance. *Anal. Chem.* **1989**, *61*, 2603-2608.

40. Bath, B. D.; Michael, D.J.; Trafton, B. J.; Joseph, J.D.; Runnels, P. L; Wightman, R. M. Subsecond adsorption and desorption of dopamine at carbon-fiber microelectrodes. *Anal. Chem.* **2000**, *72*, 5994-6002.

41. Heien, M. L. A. V.; Phillips, P. E. M.; Stuber, G. D.; Seipel, A. T.; Wightman, R. M. Overoxidation of carbon-fiber microelectrodes enhances dopamine adsorption and increases sensitivity. *Analyst* **2003**, *128*, 1413-1419.

42. Huffman, M. L.; Venton, B. J. Electrochemical properties of different carbon-fiber microelectrodes using fast-scan cyclic voltammetry. *Electroanalysis* **2008**, *20*, 2422-2428.

43. Chen, L.; Tanner, E. E. L.; Lin, C.; Compton, R. G. Impact electrochemistry reveals that graphene nanoplatelets catalyse the oxidation of dopamine via adsorption. *Chem. Sci.* **2018**, *9*, 152–159.

44. Abouelamaiem, D. I.; Mostazo-López, M. J.; He, G. J.; Patel, D.; Neville, T. P.; Parkin, I. P.; Lozano-Castelló, D.; Morallón, E.; Cazorla-Amorós, D.; Jorge, A. B.; Wang, R. F.; Ji, S.; Titirici, M. M.; Shearing, P. R.; Brett, D. J. L. New insights into the electrochemical behaviour of porous carbon electrodes for supercapacitors. *J. Energy Storage* **2018,** *19*, 337-347.

45. Viry, L.; Derre, A.; Poulin, P.; Kuhn, A. Discrimination of Dopamine and Ascorbic Acid Using Carbon Nanotube Fiber Microelectrodes. *Phys. Chem. Chem. Phys.* **2010**, *12*, 9993–9995.

46. Álvarez-Martos, I.; Ferapontova, E. E. Electrochemical label-free aptasensor for specific analysis of dopamine in serum in the presence of structurally related neurotransmitters. *Anal. Chem.* **2016**, *88*, 3608–3616.

47. Mo, J.-W.; Ogorevc, B. Simultaneous measurement of dopamine and ascorbate at their physiological levels using voltammetric microprobe based on over- oxidizedpoly(1,2-phenylenediamine)-coated carbon fiber. *Anal. Chem.* **2016**, *73*, 1196–1202.

48. Abdalla, A.; Atcherley, C. W.; Pathirathna, P.; Samaranayake, S.; Qiang, B.; Peña, E.; Morgan, S. L.; Heien, M. L.; Hashemi, P. In Vivo Ambient Serotonin Measurements at Carbon Fiber Microelectrodes. *Anal. Chem.* **2017**, *18*, 9703–9711.

TOC graphic

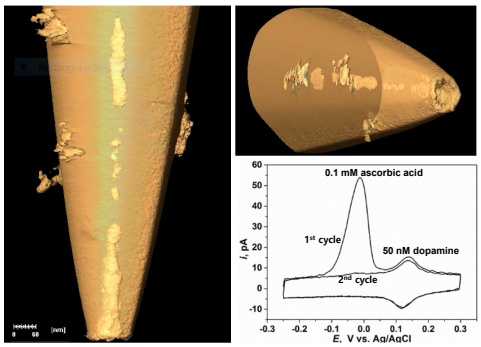
0.1 mM ascorbic acid
1st cycle
50 nM dopamine
2nd cycle
i, pA
E, V vs. Ag/AgCl